Collapse of the Mott Gap and Emergence of a Nodal Liquid in Lightly Doped Sr_2IrO_4

A. de la Torre,[1] S. McKeown Walker,[1] F. Y. Bruno,[1] S. Riccó,[1] Z. Wang,[2,1] I. Gutierrez Lezama,[1] G. Scheerer,[1] G. Giriat,[1] D. Jaccard,[1] C. Berthod,[1] T. K. Kim,[3] M. Hoesch,[3] E. C. Hunter,[4] R. S. Perry,[5] A. Tamai,[1] and F. Baumberger[1,2,6]

[1]*Department of Quantum Matter Physics, University of Geneva, 24 Quai Ernest-Ansermet, 1211 Geneva 4, Switzerland*
[2]*Swiss Light Source, Paul Scherrer Institut, CH-5232 Villigen PSI, Switzerland*
[3]*Diamond Light Source, Harwell Campus, Didcot OX11 0DE, United Kingdom*
[4]*School of Physics and Astronomy, The University of Edinburgh, James Clerk Maxwell Building, Mayfield Road,
Edinburgh EH9 2TT, United Kingdom*
[5]*London Centre for Nanotechnology and UCL Centre for Materials Discovery, University College London,
London WC1E 6BT, United Kingdom*
[6]*SUPA, School of Physics and Astronomy, University of St. Andrews, St. Andrews, Fife KY16 9SS, United Kingdom*

We report angle resolved photoemission experiments on the electron doped Heisenberg antiferromagnet $(Sr_{1-x}La_x)_2IrO_4$. For a doping level of $x = 0.05$, we find an unusual metallic state with coherent nodal excitations and an antinodal pseudogap bearing strong similarities with underdoped cuprates. This state emerges from a rapid collapse of the Mott gap with doping resulting in a large underlying Fermi surface that is backfolded by a (π, π) reciprocal lattice vector which we attribute to the intrinsic structural distortion of Sr_2IrO_4.

Superconductivity in underdoped cuprates emerges from an unusual electronic state with pseudogapped antinodal excitations coexisting with coherent nodal quasiparticles [1–3]. The relation between this state and superconductivity is intensely studied but remains controversial [4–9]. This has raised much interest in Sr_2IrO_4, a $5d$ analogue of cuprates [10–12] whose doping evolution might provide new insight into the enigmatic pseudogap phase. Sr_2IrO_4 is isostructural to La_2CuO_4 with planar IrO_2 layers forming a square lattice of Ir^{4+} ions with a nominal $5d^5$ configuration. Strong spin-orbit interaction removes the orbital degeneracy of the t_{2g} shell resulting in a single, half-filled band of spin-orbital entangled pseudospin $J_{eff} = 1/2$ states. Electron correlations cause a Mott-like insulating ground state [13,14] with (π, π) antiferromagnetic ordering and ungapped spin excitations with energies comparable to cuprates [11,15].

Besides these striking analogies, there are also notable differences between iridates and cuprates. The Coulomb repulsion in the Ir $5d$ shell is weaker leading to comparable energy scales for the charge gap and spin excitation bandwidth [16]. Further, the noninteracting Fermi surface of Sr_2IrO_4 is electronlike and centered at (0,0) [10,13], rather than holelike as in cuprates [2]. Within a Hubbard model, this suggests a particle-hole conjugate doping phase diagram with a stronger tendency towards superconductivity in electron doped Sr_2IrO_4, as pointed out in Ref. [10]. A recent numerical study, indeed, predicted d-wave superconductivity in electron doped, but not in hole doped, Sr_2IrO_4 [12]. The evolution of the microscopic electronic structure of Sr_2IrO_4 with electron doping is, therefore, of considerable interest.

Here, we report an unusual metallic state with a strong momentum anisotropy in $(Sr_{1-x}La_x)_2IrO_4$. This state bares similarities with underdoped cuprates [4–9] and emerges from a collapse of the Mott gap with doping resulting in a large Fermi surface that is broken up into disconnected arcs by an antinodal pseudogap.

Crystals of $(Sr_{1-x}La_x)_2IrO_4$ with La concentrations of $x = 0$, 0.01, and 0.05 were flux grown by standard methods. La^{3+} substitutes for Sr^{2+} [17] and proved suitable to dope electrons in layered perovskites with minimal disorder induced scattering of in-plane carriers [18]. Crucially, La doping also preserves the strong spin-orbit interaction of Ir which stabilizes the insulating ground state of the parent compound. Details of the growth and characterization of our samples are provided in the Supplemental Material [19]. For the highest doping of $x = 0.05$, $(Sr_{1-x}La_x)_2IrO_4$ shows a metallic resistivity down to ~50 K followed by an upturn at lower temperature, comparable to underdoped cuprates. We find no signs of superconductivity down to 100 mK. The magnetic ordering persists at $x = 0.01$ with slightly reduced Néel temperature while samples with $x = 0.05$ are paramagnetic. Note that, because of the stoichiometry of Sr_2IrO_4, the nominal electron doping x' on the Ir site is $2x$.

Angle-resolved photoemission spectroscopy (ARPES) measurements were performed at the I05 beam line of the Diamond Light Source. The samples were cleaved at pressures $< 10^{-10}$ mbar and temperatures < 50 K. Measurements were made using photon energies between 30 and 120 eV. All presented data were acquired at 100 eV with an energy resolution of 15 meV. The sample
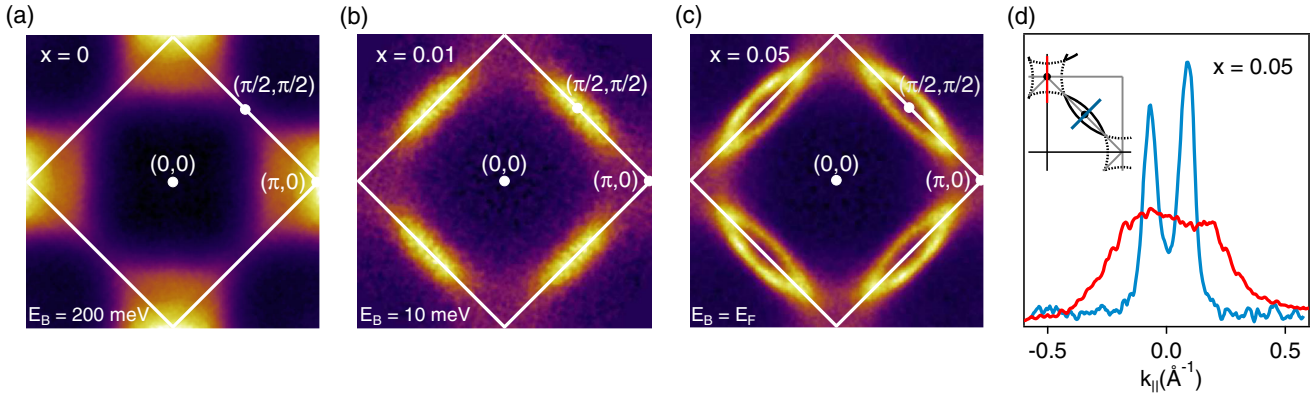
FIG. 1 (color online). Nodal liquid in lightly doped Sr_2IrO_4. (a) Constant energy contour of Sr_2IrO_4 at -200 meV showing the loci of the lowest lying charge excitations of the parent insulator in the large Brillouin zone corresponding to the Ir-Ir nearest neighbor square lattice. The white square illustrates the actual structural Brillouin zone that coincides with the magnetic zone and contains two iridium sites per plane. (b) For $x = 0.01$, the lowest lying spectral weight shifts from $(\pi, 0)$ to $(\pi/2, \pi/2)$. (c) At the higher doping of $x = 0.05$, we observe the emergence of coherent excitations along the nodal direction with clear spectral weight on the backside of the Fermi arcs. (d) Momentum distribution curves along the nodal (blue) and antinodal (red) direction illustrating the dichotomic behavior of the single particle excitations. The data in (a)–(c) have been fourfold rotationally averaged.

temperature was 8 and 50 K for conducting and insulating samples, respectively.

Figure 1 shows the evolution of the spectral weight near the Fermi level from the parent insulator ($x = 0$) to La concentrations of $x = 0.01$ and 0.05. Consistent with an earlier report on undoped Sr_2IrO_4 [13], we find the top of the lower Hubbard band (LHB) at the $(\pi, 0)$ point. Yet, already for $x = 0.01$, the low-energy spectral weight shifts to $(\pi/2, \pi/2)$ [23,24]. On increasing the doping to $x = 0.05$, coherent excitations emerge along arcs stretching out from the nodal direction, while the spectral weight along the Ir-Ir nearest neighbor direction remains weak and is devoid of sharp features, reminiscent of the nodal-antinodal dichotomy in underdoped cuprates [3,25]. However, in striking contrast to cuprates and to an earlier study on surface doped Sr_2IrO_4 [26], we find strong spectral weight on the back side of the Fermi arcs. This spectral weight is strongly photon energy dependent, as shown in the Supplemental Material, Fig. 4(b) [19] and previously observed in doped $Sr_3Ir_2O_7$ [27]. In order to understand this Fermi surface, it is important to recall the significant rotation of the octahedra in bulk Sr_2IrO_4. This causes a doubling of the unit cell and, thus, back folding into a small Brillouin zone that coincides with the magnetic zone [28]. Considering that equally strong back folding was observed previously in isostructural and nonmagnetic Sr_2RhO_4 [29], it is compelling to attribute the reduced momentum-space periodicity predominantly to a structural effect.

Thus, we turn our attention to the more fundamental issue of a small versus large Fermi surface. A small Fermi surface comprising the doped carriers was recently reported for the La doped bilayer iridate $Sr_3Ir_2O_7$, which shows characteristics of a correlated doped semiconductor and exhibits highly coherent quasiparticle states along the entire

Fermi surface [30]. On the other hand, a large Fermi surface of volume $1 + x'$ is observed in cuprates and is expected if all electrons in a doped single-band Mott insulator contribute to the Luttinger volume. This question cannot be decided reliably based on the enclosed Fermi surface volume alone. For $x = 0.05$, the difference between a large circular Fermi surface centered at $(0,0)$ and four lenslike small Fermi pockets at $(\pi/2, \pi/2)$ is small and within the range of deviations from Luttinger's theorem observed in cuprates. Thus, it is essential to follow the evolution of the LHB with doping, which was not possible on surface doped Sr_2IrO_4 [26]. To this end, we compare, in Fig. 2, the band dispersion of $(Sr_{1-x}La_x)_2IrO_4$ for $x = 0$ and $x = 0.05$.

In undoped Sr_2IrO_4, the electronic structure is dominated by gapped holelike bands with maxima at $(0,0)$, $(\pi, 0)$, and $(\pi/2, \pi/2)$ as shown by blue markers in Fig. 2(g). For clarity, we describe the dispersion of these bands by a tight binding (TB) calculation that includes spin-orbit (SO) interaction and Coulomb repulsion (TB + SO + U) [31]. The latter is treated self-consistently in a mean field expansion of the density operator n and, thus, cannot account for the different ways in which bands of different pseudospin characters are affected by electronic correlations. Despite the limitations of the model in handling correlations, we observe a good qualitative agreement between the calculated and the experimental dispersions for the parent compound using realistic parameters for the spin-orbit interaction ($\lambda = 0.57$ eV) and Coulomb repulsion ($U = 2$ eV). Full details of this model are given in the Supplemental Material [19]. Projecting the wave functions onto a pseudospin basis, we find $J_{eff} = 1/2$ states at $(\pi, 0)$ and $(\pi/2, \pi/2)$ while the band with similar energy at $(0,0)$ is of $J_{eff} = 3/2$ character.
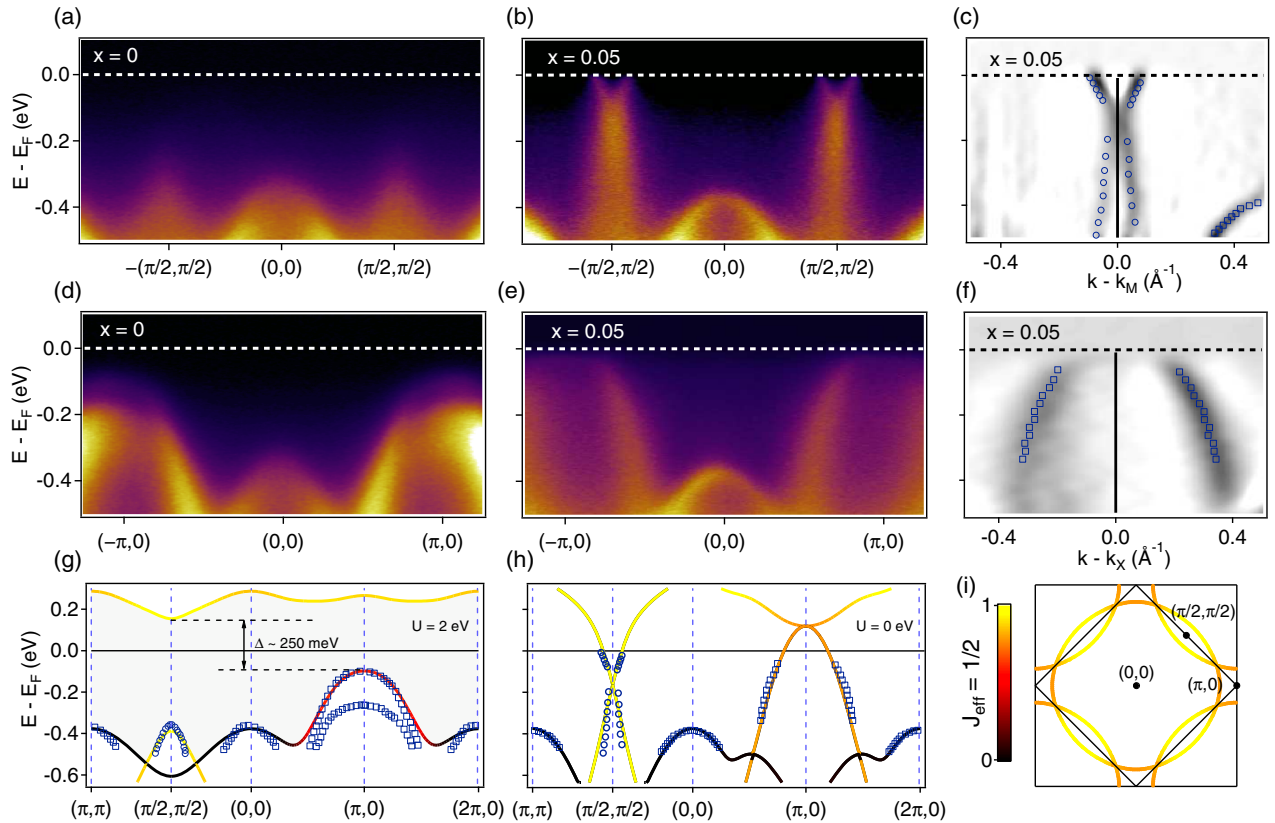
FIG. 2 (color online).   Collapse of the Mott gap. (a),(d) Photoemission intensity in the fully gapped parent insulator along the nodal and antinodal direction, respectively. (b),(e) For $x = 0.05$, electronlike metallic states appear at $(\pi/2, \pi/2)$ while the apex of the holelike band at $(\pi, 0)$ moves above the chemical potential resulting in a collapse of the charge gap. (c),(f) Curvature plots of the raw data used to extract band positions. (g) Band dispersion for $x = 0$ compared to a TB + SO + U calculation. (h) Band dispersion for $x = 0.05$ compared to a calculation with $U = 0$. Square (circular) symbols indicate data points extracted from two-dimensional (one-dimensional momentum) curvature plots. (i) Large electronlike Fermi surface corresponding to the TB calculation with $U = 0$ and comprising $1 + x'$ carriers. The color scale in (g)–(i) encodes pseudospin $J_{\mathrm{eff}} = 1/2$ character.

Upon La doping, marked changes in the $J_{\mathrm{eff}} = 1/2$ dispersion occur. Most notably, around $(\pi/2, \pi/2)$ bands with nearly linear dispersion appear at the Fermi level. For $x = 0.05$, these bands extrapolate to a Dirac point around -0.1 eV and continue to disperse quasilinearly at higher energy, although we cannot presently exclude a small gap along the high-symmetry line. Along the antinodal direction, the holelike $J_{\mathrm{eff}} = 1/2$ band at $(\pi, 0)$ shifts towards the chemical potential and clearly extrapolates to a band apex above the Fermi level [Figs. 2(e) and 2(f)]. Hence, the Mott gap is fully collapsed for this doping level. The $J_{\mathrm{eff}} = 3/2$ bands, on the other hand, are not affected strongly by doping. This behavior is summarized in Fig. 2(h) where we show band positions for $x = 0.05$ extracted from curvature plots of the raw data [see Figs. 2(c) and 2(f) and Supplemental Material [19]]. Clearly, this electronic structure cannot be described by a rigid shift of the tight binding band structure that describes the parent compound. Instead, we find that the band dispersion for $x = 0.05$ is well approximated by a calculation with $U = 0$ describing a weakly interacting metallic state which, by construction,

has $1 + x'$ itinerant carriers per Ir site and, thus, corresponds to a large Fermi surface [see Fig. 2(i)]. Thus, the low-energy excitations in doped iridates share a key property of the first doped holes in cuprates. They both track the noninteracting band structure [32]. Even the nodal Fermi velocity of $\sim 10^5$ m/s in iridates is similar to lightly doped cuprates [3,33]. However, the collapse of the Mott state is far more pronounced and rapid in iridates where already, at $x = 0.05$, no trace of the lower Hubbard band remains. This is distinct from cuprates where the evolution from insulator to strange metal proceeds more gradually via a progressive transfer of spectral weight from the Hubbard band to the coherent quasiparticle band [32]. While a profound understanding of this difference will require further theoretical work, we speculate that it reflects a reduced Mottness of Sr_2IrO_4 arising from the weaker Coulomb repulsion in the $5d$ shell.

Back folding of the large Fermi surface by the (π, π) wave vector of the structural distortion breaks the single circular Fermi surface into lenslike electron pockets and nearly square hole pockets. Within our tight-binding

model, a small gap can be opened between these pockets by including a finite U (see Supplemental Material, Fig. 6 [19]). A very small band gap is also observed in Density Functional Theory calculations for undoped Sr_2IrO_4 with $U = 0$ and assuming an $I4_1/acd$ crystal structure [14]. However, even if such a gap is present, the Fermi surface still contains $1 + x'$ carriers per site and is, thus, large by this definition. More importantly, a possible small band gap at the Brillouin zone boundary does not push the hole band at the $(\pi, 0)$ point below the chemical potential [14], as it is observed in electron doped $Sr_3Ir_2O_7$ [30]. Hence, the suppression of the spectral weight along the antinodal direction described in Fig. 1 cannot be explained by a single particle band gap. Instead, it is indicative of a momentum dependent pseudogap.

Direct evidence for a pseudogap is summarized in Fig. 3. Energy distribution curves along the node [Fig. 3(a)] show small quasiparticlelike peaks with a sharp cutoff at the Fermi level, while the low-energy spectral weight is clearly suppressed along the antinode [Fig. 3(b)]. In order to quantify the anisotropy of the pseudogap, we fit particle-hole symmetrized Energy Distribution Curves along the large Fermi surface with the Dynes function [34] often used to quantify superconducting gaps. While this procedure is purely phenomenological and cannot give absolute gap values, it is still suitable for monitoring the evolution of the pseudogap with momentum. For $x = 0.05$, where the spectral weight has a well defined cutoff along the entire Fermi surface, we find no significant pseudogap near the node within the accuracy of the experiment of approximately 3 meV. Moving out along the Fermi surface towards the

antinode, the pseudogap starts to open at a Fermi surface angle of $\sim 15°$ for the main band and possibly slightly earlier for the backfolded band. As shown in Fig. 3(d), this angle is smaller than the crossing with the Brillouin zone boundary demonstrating that, already, the lenslike part of the Fermi surface is broken into two disconnected arcs and a small gapped region near the apex. Elucidating the precise doping range over which this behavior exists will require further detailed measurements. For $x = 0.01$, the suppression of spectral weight has a less clearly defined onset in energy. However, consistent with the insulating nature of this sample, a pseudogap is clearly present along the entire Fermi surface and reaches values up to ~ 80 meV near the antinode (see Supplemental Material, Fig. 3 [19]).

The origin of the pseudogap in Sr_2IrO_4 cannot be determined unambiguously from our present data. In cuprates, a pseudogap with strikingly similar phenomenology is often associated with preformed nonphase coherent pairs [1,8] or competing ordered states [7]. Yet, the pseudogap in Sr_2IrO_4 persists above 100 K, while our samples show no superconductivity down to 100 mK at a doping level of $x' = 0.1$ where hole doped cuprates are superconducting. Moreover, neither our ARPES data nor diffraction experiments [16,28] give evidence of competing ordered states as they are found by different techniques in the pseudogap phase of cuprates [4,6,7]. Thus, our results suggest that the anisotropic pseudogap observed here is not a manifestation of preformed pairs or competing ordered states. This raises the question whether an antinodal pseudogap is an intrinsic property of lightly doped low-dimensional Mott insulators with Heisenberg
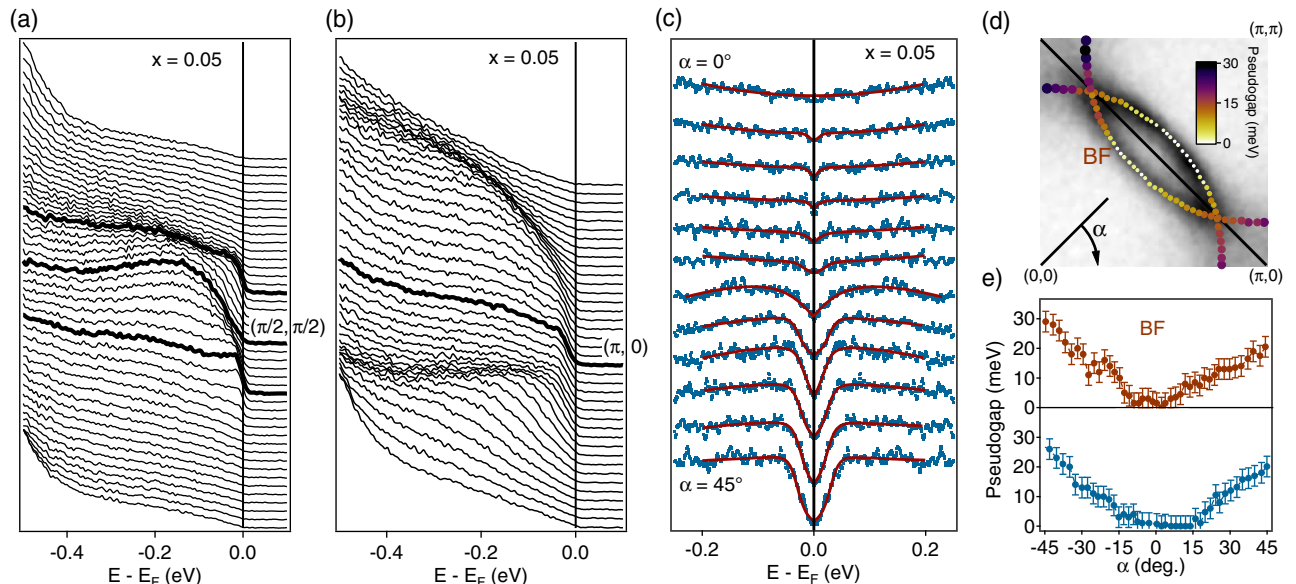

FIG. 3 (color online).   Anisotropic pseudogap for $x = 0.05$. (a),(b) Energy distribution curves along $(0, 0) - (\pi, \pi)$ and $(0, 0) - (\pi, 0)$, respectively, showing a suppression of the low-energy spectral weight in the antinodal region [panel (b)]. (c) Symmetrized Energy Distribution Curves (blue dots) and fits to the Dynes formula (red lines) for different angles along the Fermi surface. (d) Fermi surface with the color-coded magnitude of the pseudogap overlaid. Note that the onset of the pseudogap is observed slightly before the apex of the lenslike contour. (e) Pseudogap value for the original (blue markers) and back folded (BF) (red markers) band as a function of Fermi surface angle.

[1] M. R. Norman, H. Ding, M. Randeria, J. C. Campuzano, T. Yokoya, T. Takeuchi, T. Takahashi, T. Mochiku, K. Kadowaki, P. Guptasarma, and D. G. Hinks, Nature (London) **392**, 157 (1998).

[2] A. Damascelli, Z. Hussain, and Z.-X. Shen, Rev. Mod. Phys. **75**, 473 (2003).

[3] K. Shen, F. Ronning, D. Lu, F. Baumberger, N. Ingle, W. Lee, W. Meevasana, Y. Kohsaka, M. Azuma, M. Takano, H. Takagi, and Z.-X. Shen, Science **307**, 901 (2005).

[4] T. Hanaguri, C. Lupien, Y. Kohsaka, D.-H. Lee, M. Azuma, M. Takano, H. Takagi, and J. Davis, Nature (London) **430**, 1001 (2004).

[5] T. Kondo, R. Khasanov, T. Takeuchi, J. Schmalian, and A. Kaminski, Nature (London) **457**, 296 (2009).

[6] G. Ghiringhelli, M. Le Tacon, M. Minola, S. Blanco-Canosa, C. Mazzoli, N. B. Brookes, G. M. De Luca, D. G. Frano, A. Hawthorn, F. He, T. Loew, M. Moretti Sala, D. C. Peets, M. Salluzzo, E. Schierle, R. Sutarto, G. A. Sawatzky, E. Weschke, B. Keimer, and L. Braicovich, Science **337**, 821 (2012).

[7] R. Comin, A. Frano, M. M. Yee, Y. Yoshida, H. Eisaki, E. Schierle, E. Weschke, R. Sutarto, F. He, A. Soumyanarayanan, Y. He, M. Le Tacon, I. S. Elfimov, J. E. Hoffman, G. A. Sawatzky, B. Keimer, and A. Damascelli, Science **343**, 390 (2014).

[8] T. Kondo, Y. Hamaya, A. D. Palczewski, T. Takeuchi, J. S. Wen, Z. J. Xu, G. Gu, J. Schmalian, and A. Kaminski, Nat. Phys. **7**, 21 (2011).

[9] M. R. Norman, D. Pines, and C. Kallin, Adv. Phys. **54**, 715 (2005).

[10] F. Wang and T. Senthil, Phys. Rev. Lett. **106**, 136402 (2011).

[11] J. Kim, D. Casa, M. H. Upton, T. Gog, Y.-J. Kim, J. F. Mitchell, M. van Veenendaal, M. Daghofer, J. van den Brink, G. Khaliullin, and B. J. Kim, Phys. Rev. Lett. **108**, 177003 (2012).

[12] H. Watanabe, T. Shirakawa, and S. Yunoki, Phys. Rev. Lett. **110**, 027002 (2013).

[13] B. J. Kim, H. Jin, S. J. Moon, J. Y. Kim, B. G. Park, C. S. Leem, J. Yu, T. W. Noh, C. Kim, S. J. Oh, J. H. Park, V. Durairaj, G. Cao, and E. Rotenberg, Phys. Rev. Lett. **101**, 076402 (2008).

[14] C. Martins, M. Aichhorn, L. Vaugier, and S. Biermann, Phys. Rev. Lett. **107**, 266404 (2011).

[15] G. Jackeli and G. Khaliullin, Phys. Rev. Lett. **102**, 017205 (2009).

[16] S. Fujiyama, H. Ohsumi, T. Komesu, J. Matsuno, B. J. Kim, M. Takata, T. Arima, and H. Takagi, Phys. Rev. Lett. **108**, 247212 (2012).

[17] M. Ge, T. F. Qi, O. B. Korneta, D. E. De Long, P. Schlottmann, W. P. Crummett, and G. Cao, Phys. Rev. B **84**, 100402(R) (2011).

[18] K. M. Shen, N. Kikugawa, C. Bergemann, L. Balicas, F. Baumberger, W. Meevasana, N. J. C. Ingle, Y. Maeno, Z. X. Shen, and A. P. Mackenzie, Phys. Rev. Lett. **99**, 187001 (2007).

[19] See Supplemental Material at http://link.aps.org/supplemental/10.1103/PhysRevLett.115.176402 for sample information and additional data, which includes [20–22].

[20] J.-M. Carter, V. Shankar, and H.-Y. Kee, Phys. Rev. B **88**, 035111 (2013).

[21] P. Zhang, P. Richard, T. Qian, Y.-M. Xu, X. Dai, and H. Ding, Rev. Sci. Instrum. **82**, 043712 (2011).

[22] M. K. Crawford, M. A. Subramanian, R. L. Harlow, J. A. Fernandez-Baca, Z. R. Wang, and D. C. Johnston, Phys. Rev. B **49**, 9198 (1994).

[23] V. Brouet, J. Mansart, L. Perfetti, C. Piovera, I. Vobornik, P. Le Fèvre, F. Bertran, S. C. Riggs, M. C. Shapiro, P. Giraldo-Gallo, and I. R. Fisher, Phys. Rev. B **92**, 081117 (2015).

[24] M. Y. Li, Z. T. Liu, F. H. Yang, J. L. Zhao, Q. Yao, C. C. Fan, J. S. Liu, B. Gao, D. W. Shen, and X. M. Xie, Chin. Phys. Lett. **32**, 057402 (2015).

[25] X. J. Zhou, T. Yoshida, D.-H. Lee, W. L. Yang, V. Brouet, F. Zhou, W. X. Ti, J. W. Xiong, Z. X. Zhao, T. Sasagawa, T. Kakeshita, H. Eisaki, S. Uchida, A. Fujimori, Z. Hussain, and Z.-X. Shen, Phys. Rev. Lett. **92**, 187001 (2004).

[26] Y. K. Kim, O. Krupin, J. D. Denlinger, A. Bostwick, E. Rotenberg, Q. Zhao, J. F. Mitchell, J. Allen, and B. J. Kim, Science **345**, 187 (2014).

[27] J. He, H. Hafiz, T. R. Mion, T. Hogan, C. Dhital, X. Chen, Q. Lin, M. Hashimoto, D. H. Lu, Y. Zhang, R. S. Markiewicz, A. Bansil, S. D. Wilson, and R.-H. He, Sci. Rep. **5**, 8533 (2015).

[28] J. W. Kim, Y. Choi, J. Kim, J. F. Mitchell, G. Jackeli, M. Daghofer, J. van den Brink, G. Khaliullin, and B. J. Kim, Phys. Rev. Lett. **109**, 037204 (2012).

[29] F. Baumberger, N. J. C. Ingle, W. Meevasana, K. M. Shen, D. H. Lu, R. S. Perry, A. P. Mackenzie, Z. Hussain, D. J. Singh, and Z. X. Shen, Phys. Rev. Lett. **96**, 246402 (2006).

[30] A. de la Torre, E. C. Hunter, A. Subedi, S. McKeown-Walker, A. Tamai, T. K. Kim, M. Hoesch, R. S. Perry, A. Georges, and F. Baumberger, Phys. Rev. Lett. **113**, 256402 (2014).

[31] H. Jin, H. Jeong, T. Ozaki, and J. Yu, Phys. Rev. B **80**, 075112 (2009).

[32] K. M. Shen, F. Ronning, D. H. Lu, W. S. Lee, N. J. C. Ingle, W. Meevasana, F. Baumberger, A. Damascelli, N. P. Armitage, L. L. Miller, Y. Kohsaka, M. Azuma, M. Takano, H. Takagi, and Z. X. Shen, Phys. Rev. Lett. **93**, 267002 (2004).

[33] A. Ino, C. Kim, M. Nakamura, T. Yoshida, T. Mizokawa, A. Fujimori, Z.-X. Shen, T. Kakeshita, H. Eisaki, and S. Uchida, Phys. Rev. B **65**, 094504 (2002).

[34] R. C. Dynes, V. Narayanamurti, and J. P. Garno, Phys. Rev. Lett. **41**, 1509 (1978).

[35] C. Huscroft, M. Jarrell, T. Maier, S. Moukouri, and A. N. Tahvildarzadeh, Phys. Rev. Lett. **86**, 139 (2001).

[36] O. Parcollet, G. Biroli, and G. Kotliar, Phys. Rev. Lett. **92**, 226402 (2004).

[37] M. Ferrero, P. S. Cornaglia, L. De Leo, O. Parcollet, G. Kotliar, and A. Georges, Phys. Rev. B **80**, 064501 (2009).